Sensor and Simulation Notes

Note 450

November 2000

Experimental Results of Optimizing the Location of Feed Arms in a Collapsible IRA and a Solid IRA

Leland H. Bowen and Everett G. Farr
Farr Research, Inc.

Carl E. Baum, Tyrone C. Tran, and William D. Prather
Air Force Research Laboratory, Directed Energy Directorate

Abstract

In Sensor and Simulation Note 438, J. Scott Tyo developed a method of optimizing the feed arm geometry for a 4-arm IRA with an arbitrarily specified input impedance. In this paper we implement this method to optimize two IRAs, a solid IRA with a 46 cm (18 inch) diameter, and a collapsible IRA with a 1.22 meter (48 in) diameter. Models of each design are built and tested with feed arms located at ±30 degrees from the angle of dominant polarization of the antenna. The RF characteristics of the two antennas are compared before and after optimization. In both cases, optimization of the feed arm geometry improved both the gain and the crosspol rejection of the antennas. A mild side effect was a slight increase in TDR reflections at the end of the feed arms.

This work was funded in part by the Air Force Office of Scientific Research, Alexandria, VA, and in part by the Air Force Research Laboratory, Directed Energy Directorate, under contract F29601-00-C-0045.

I. Introduction.

A method of optimizing the placement of the feed arms of an Impulse Radiating Antenna (IRA) has recently been described by J. Scott Tyo [1]. The objective of this optimization is to increase the antenna gain by adjusting the placement of the feed arms. The concept of adjusting feed arm placement was previously suggested by C. E. Baum in [2]. In this paper, we demonstrate experimentally the validity of the technique with two IRAs, a solid IRA, and a collapsible IRA.

In [1], Tyo described the optimization of the feed arm geometry for IRAs with four coplanar plate feed arms. The standard IRA configuration is symmetric, with the feed arms perpendicular to each other or, in other words, at ±45° from the vertical. (The dominant polarization of the antenna is assumed to be vertical in this paper.) Tyo's results indicate that the prompt aperture efficiency (proportional to power – not voltage) can be increased from ~25% for the ±45° case to ~35% for the optimum configuration. The results in [1] can be used to optimize a 4-arm IRA with an arbitrarily specified input impedance. In this paper we consider only IRAs with a nominal 200 Ω impedance at the input to the feed arms. For this case, the results of [1] give an optimum angle of about ±23° from vertical. At this angle the feed arms are very wide, making it difficult to maintain a flat TDR at the end of the feed arms. So for the antennas described here, the feed arms are placed at ±30° from the vertical. This compromise provides a gain that is nearly optimal, without letting the feed arms to get too wide.

We compare the results with the feed arms at ±45° and at ±30° from the vertical for two IRAs designed and built by Farr Research, Inc. The first antenna is built using an 46 cm (18 in) diameter aluminum reflector and the second is a Collapsible IRA (CIRA) with a 1.22 m (48 in) diameter reflector made of conductive fabric on an umbrella like frame. In both cases, moving the feed arms from ±45° to ±30° improved the effective gain, aperture efficiency, and crosspol rejection. Although crosspol rejection is not an optimization parameter, the reduction in the horizontal component of the feed arms is expected to reduce the coupling of horizontal electric fields to the antenna.

The antenna measurements presented in this report were made using the outdoor time domain antenna range at Farr Research. The time domain results are converted to the frequency domain using the procedure given in [3]. In [1], the aperture height divided by the aperture radius (h_a/a) is used as the optimization parameter. Therefore, we will also use this parameter for comparisons in this report. We can calculate h_a from the integral of the normalized impulse response using equations 3.3 and 7.4 of [3]

$$h_{a,RX} = \frac{\sqrt{f_{g,RX}}}{\tau_{p,RX}} \int_{\text{Impulse}} h_{N,RX}(t)\, dt \qquad (1)$$

where $\tau_{p,RX} = 1$ for a perfect balun and $f_{g,RX} = Z_c/Z_o = 50\ \Omega / 377\ \Omega$.

Another parameter of interest for comparing IRAs is the effective gain, which is just the antenna gain reduced by the return loss. As stated in [4], the argument for using effective gain is that impedance mismatches are an integral part of an antenna's response, and therefore should be included. We will show that for both antenna designs the effective gain is considerably improved in the ±30° designs, when compared to the ±45° designs.

II. Solid IRA.

The IRA-1 has an 46 cm (18 in) diameter aluminum reflector with a F/D of 0.5. The feed arms on this antenna are spaced at 90° increments or ±45° from the vertical, as is standard for the traditional IRA. The splitter located on the back of the reflector has two 100 Ω semi-rigid cables connected in parallel. We show the RF characteristics of the IRA-1 in the left-hand column of plots below. The initial development of the IRA-1 was described in [5].

Based on information in [1], we redesigned the IRA-1 so that the feed arms are at ±30° rather than ±45° as used in the past. This change resulted in a greatly improved version of the IRA that we call IRA-2. We show the measurements for the IRA-2 in the right-hand column of plots below. Photographs of the two IRAs are shown in Figure 2.1. The feed arms for the IRA-1 have an included angle of 13.6°and for the IRA-2 the included angle is 23.2°. The load resistance for each feed arm is made up of two 400 Ω high voltage resistors mounted in parallel on a small circuit card. The load resistors are manufactured by Advanced Power Components.

The TDRs of the antennas are shown in Figure 2.2. The TDR of the feed point of the IRA-2 is somewhat better than that of the IRA-1. We continue to make slight improvements in the construction of the antennas, especially at the feed point. Both antennas have a dip in the impedance in the region of the load resistors. This dip is due in part to the electric field incident on the center of the parabolic reflector at time F/c where c is the speed of light in free space. The reflected field has a ramp-function time dependence, and is apparent in the TDR as a negative dip at time $2F/c$ [8]. The configuration of the circuit card and the physical size of the resistors also contribute to the dip in the impedance. We have discovered methods of improving the impedance match in this region for both designs. These methods involve the use of distributed resistors for the ±45° design, and the use of a small inductance at the end of the feed arm for the ±30° design. These methods will be reported in a future Sensor and Simulation Note.

The boresight measurements and the normalized impulse responses are shown in Figures 2.3–2.6. The measurements reported here were made using a FRI-TEM-01-50 sensor as the source antenna and the IRA as the receiver. The distance between the apertures was 10 m. The sensor characteristics are given in [6]. Both antennas have outstanding electrical characteristics in both the frequency and time domains. In the time domain, the FWHM of impulse response is 37 ps for the IRA-1 and 33 ps for the IRA-2. In the frequency domain, the peak effective gain at 15 GHz is about 26 dBi for the IRA-1 and 29 dBi for the IRA-2. The IRA-2 has a frequency range of 100 MHz to 20 GHz as shown in Figure 2.7.

From Figure 2.5 we get h_a/a = 0.524 for the IRA-1 and 0.624 for the IRA-2. This indicates an improvement of 19% which is greater than expected. However, the values for h_a/a from Figure 10 of [1] are 0.65 for the ±45° case and 0.75 for the ±30° case so we see that our measurements do not exceed the theoretical values. Part of the improvement in the IRA-2 is probably due to slight improvements in the feed point construction.

Finally, we provide the crosspol response in Figures 2.8–2.9. The IRA-2 has a minimum crosspol rejection of 17 dB across the band. This is an improvement of 11 dB over the IRA-1, which is quite a bit better than we had expected.

Figure 2.1. IRA-1 with feed arms at ±45° (left) and IRA-2 with feed arms at ±30° (right).

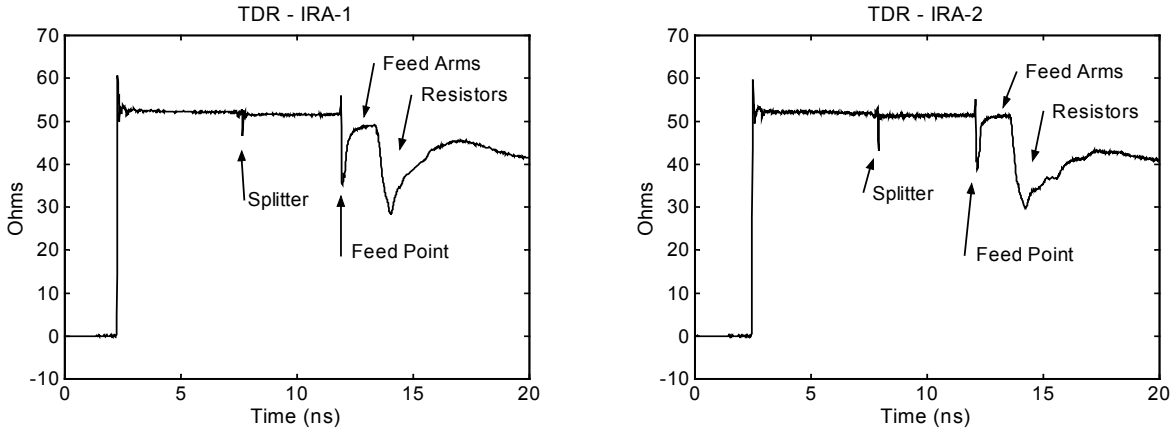

Figure 2.2. TDR of IRA-1 and IRA-2.

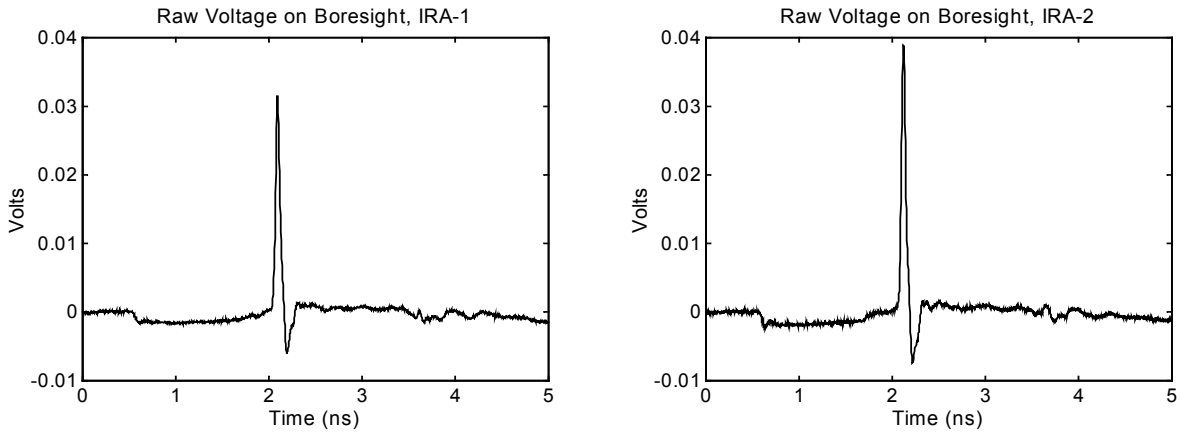

Figure 2.3. Raw voltage on boresight at 10m.

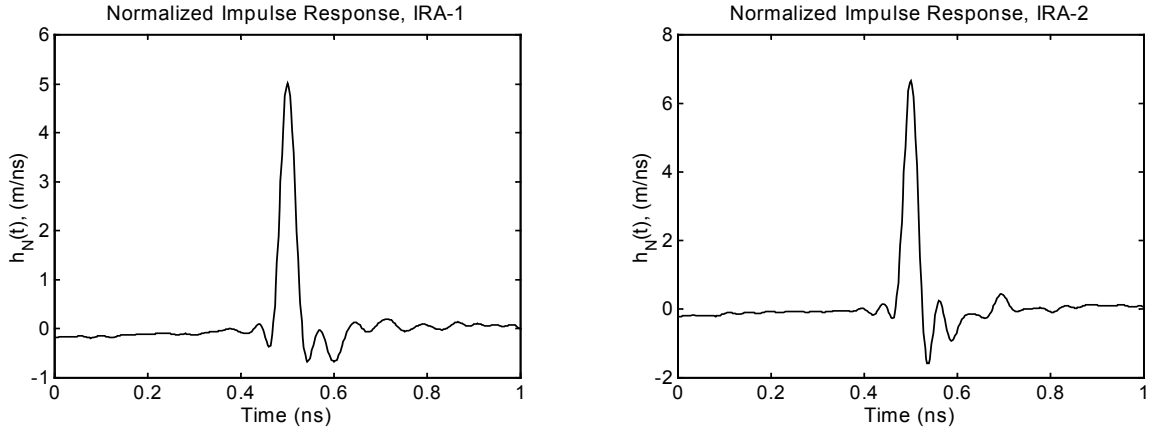

Figure 2.4. Normalized Impulse Response in the time domain.

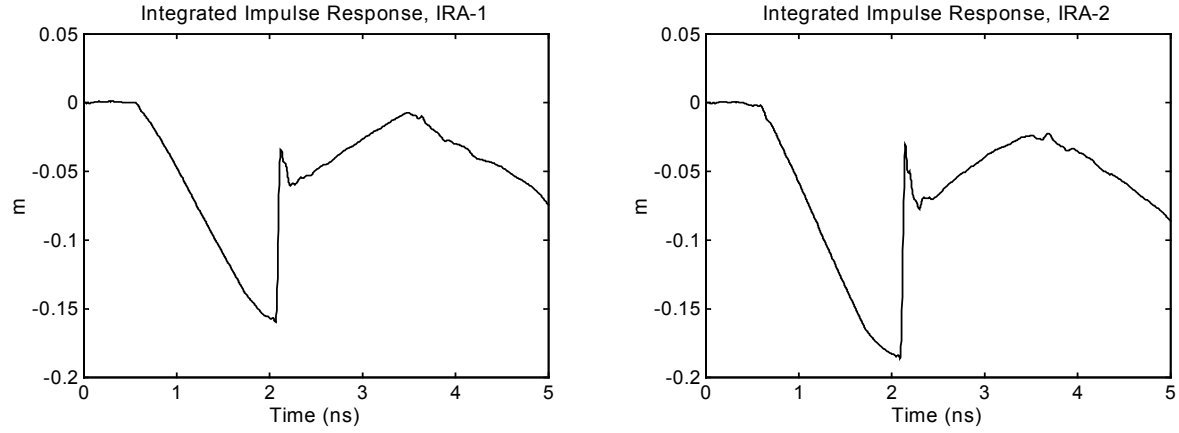

Figure 2.5. Integral of the Impulse Response (h_a).

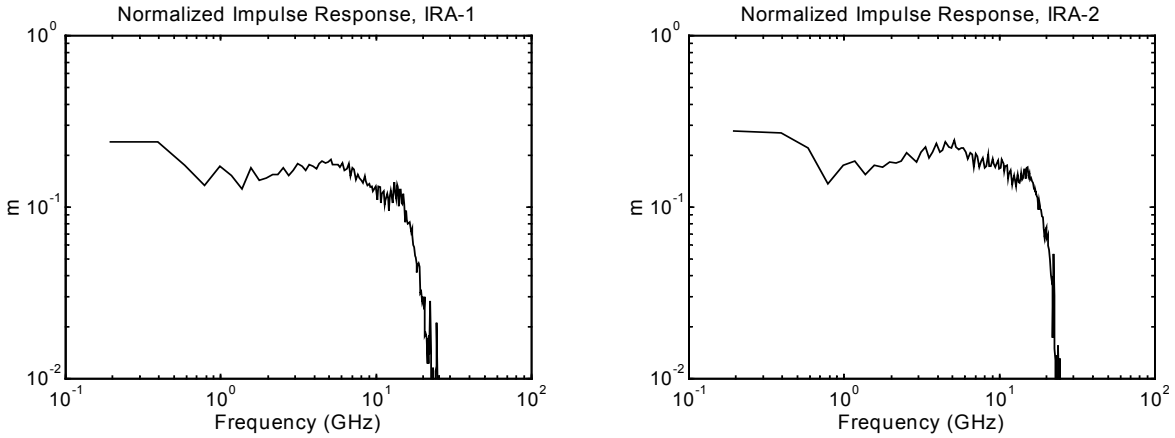

Figure 2.6. Normalized Impulse Response in the frequency domain.

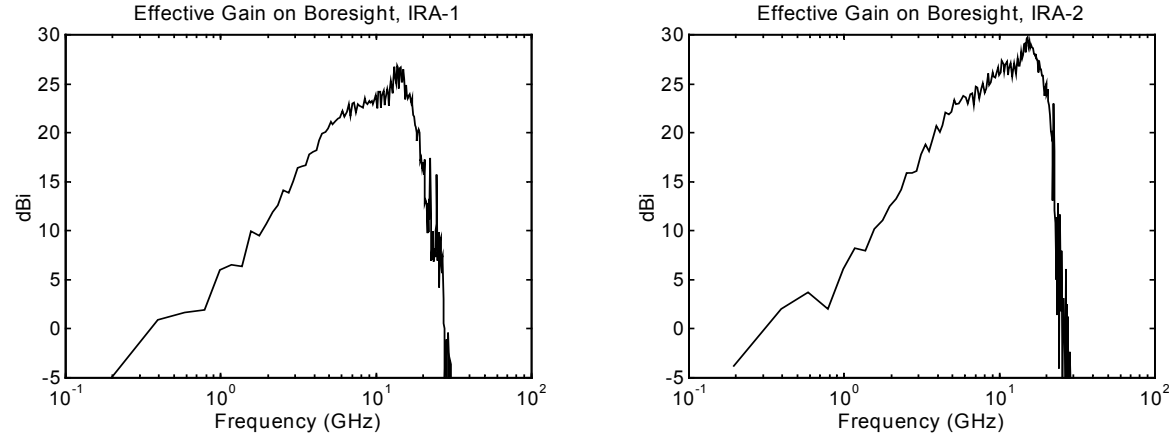

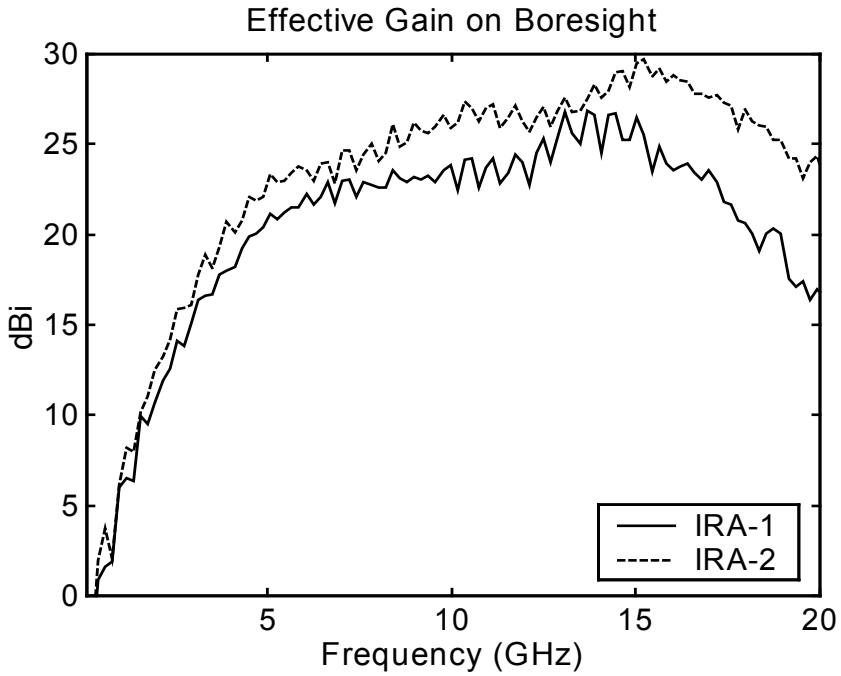

Figure 2.7. Effective gain on boresight.

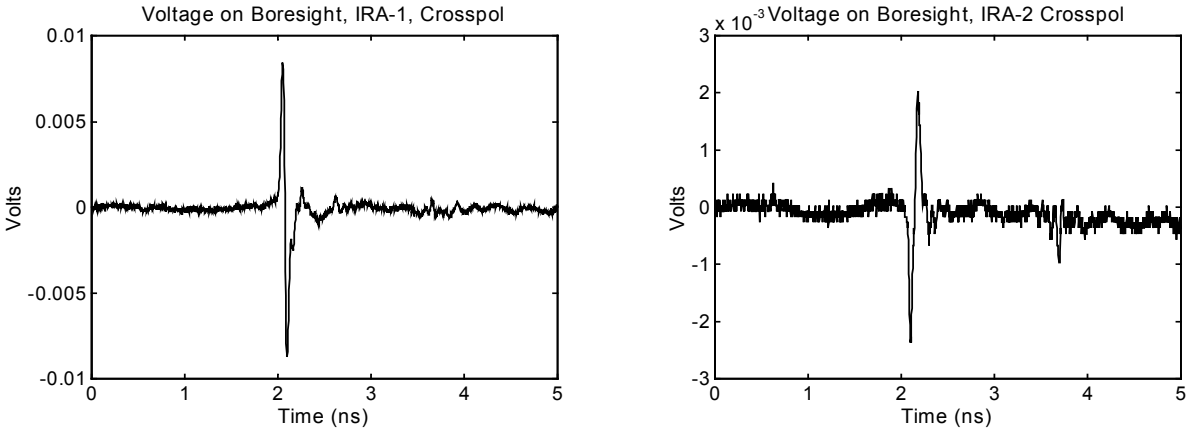

Figure 2.8. Cross polarization response on boresight.

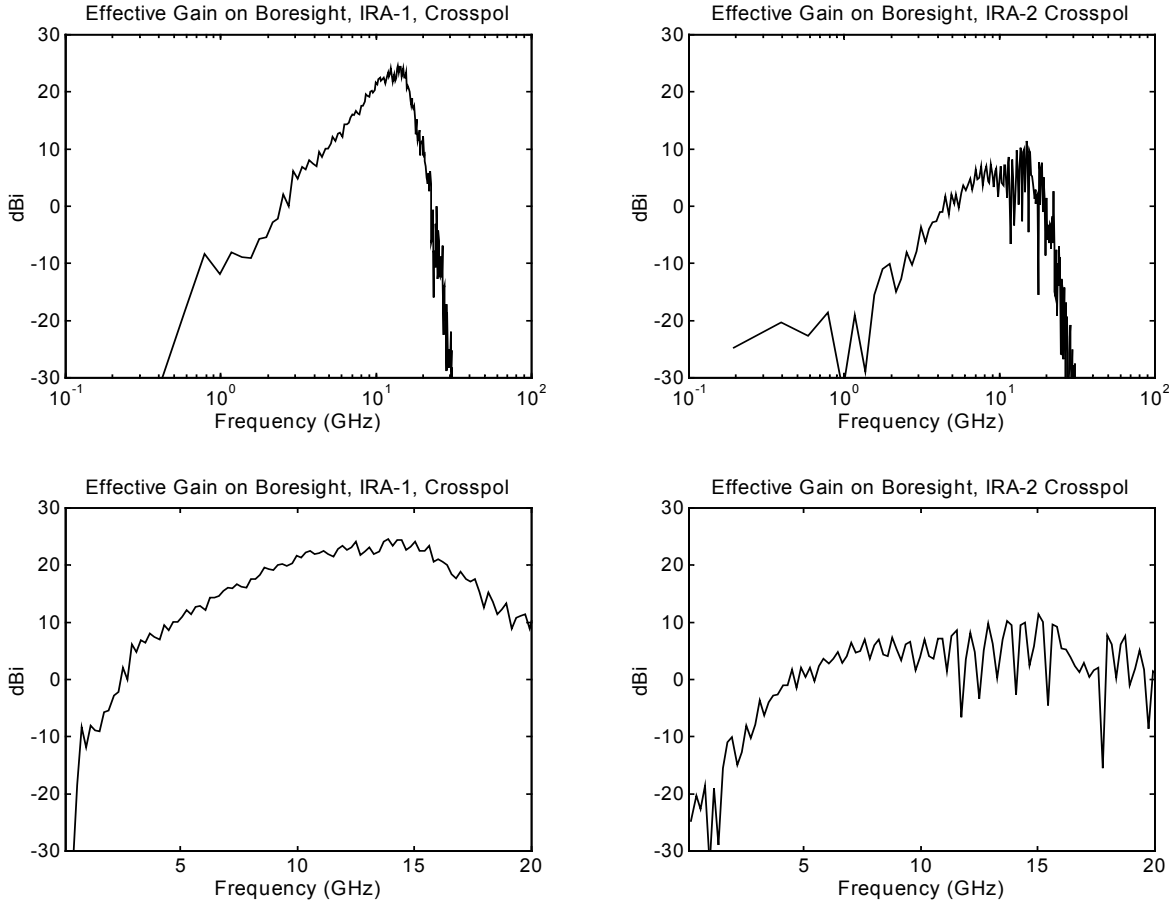

Figure 2.9. Cross polarization gain on boresight.

III. Collapsible IRA (CIRA).

The design of the CIRA is based on a 1.22 m (48 in) diameter parabolic dish with a focal length of 0.488 m (F/D = 0.4) [6]. The reflector for the collapsible antenna is sewn from 12 panels made of a very tough conductive mesh fabric. The reflectors are supported on a frame of fiberglass rods attached to an aluminum center housing by aluminum pivots or hinges. The feed arms are made from a combination of conductive and resistive fabrics. The splitter consists of a 50 Ω input impedance connector, which then splits into two 95 Ω flexible cables. The cables attach to the feed arms at the feed point in a series/parallel configuration as is standard for IRAs with 4 feed arms. The collapsed antenna measures 102 mm (4 in.) diameter x 810 mm (32 in.) long. The antenna weighs 2 kg (4.5 lb.). The CIRA was designed to be man-portable, so weight and size are important parameters. The CIRA-1, which has the feed arms at ±45°, is described more fully in [6]. The CIRA-2 has the feed arms at ±30°. Since the cables from the splitter are 95 Ω, the feed arms must be matched to 190 Ω for the CIRAs rather than 200 Ω as for the IRAs. With the 190 Ω impedance and F/D of 0.4, we get an included angle of 18.1° for the ±45° case and 30.5° for the ±30° case. Both antennas are shown in Figure 3.1. The larger included angle required for the feed arms in the ±30° case makes the area of the feed arms quite large, as seen in the picture of the CIRA-2 (Figure 3.1).

The TDRs of the two antennas are shown in Figure 3.2. The TDR of the CIRA-1 is quite flat overall. The small bumps in the area of the load resistors are due to the reverse taper of the feed arms in this area. The CIRA-2 has a dip in the impedance in the region of the load resistors. The cause of this dip and means of improving the impedance match in this region are interesting subjects which we plan to discuss in a later Sensor and Simulation Note. As mentioned earlier, methods of improving the impedance match in this region have been determined. However, they may be difficult to implement on the fabric feed arms of the CIRA.

The boresight measurements and the normalized impulse responses are shown in Figures 3.3–3.6. The measurements for the CIRA-1 were made using a FRI-TEM-02-100 sensor and the measurements for the CIRA-2 were made using a FRI-TEM-01-50 sensor. While it would have been preferable to use the same sensor in both sets of data, it does not matter, because the sensor response is deconvolved from the data. Furthermore, it has been shown previously in [6] that measurements with the two different sensors give the same result after compensation anyway. The characteristics of both sensors are given in Section II of [6]. The distance between the apertures of the source antenna and the CIRAs was 20 m for the measurements given here. As stated in [6], it would have been better to use a distance of 25 m, however, there was no opportunity to make measurements at a greater distance, and we believe the errors in the measurements are small. Both antennas have outstanding RF characteristics in both the frequency and time domains. In the time domain, the FWHM of impulse response is 73 ps for the CIRA-1 (68 ps using the TEM-1-50) and 70 ps for the CIRA-2. In the frequency domain, the peak gain is about 23 dBi at 5 GHz for the CIRA-1 and 24 dBi at 9 GHz for the CIRA-2. The CIRA-2 is usable from about 100 MHz to 12 GHz as shown in Figure 3.6.

From Figure 3.5 we get h_a/a = 0.446 for the IRA-1 and 0.451 for the IRA-2. This indicates an improvement of 1.1% which is not as good as expected. The values for h_a/a from Figure 10 of (1) are 0.64 for the ±45° case and 0.73 for the ±30° case. The fact that our measurements are below the theoretical values is due largely to the fabric reflector not being a

true paraboloid. Nevertheless, the effective gain is significantly improved in the CIRA-2 with respect to the CIRA-1, as shown in Figure 3.7.

Finally, we provide the crosspol response in Figures 3.8–3.9. The CIRA-1 has a crosspol rejection of from 5 to 20 dB. The CIRA-2 has approximately 5 dB more crosspol rejection than the CIRA-1. The improvement in both gain and crosspol rejection for the CIRA is not as great as seen in the IRA. However, the effect of the optimization is still significant.

Figure 3.1. CIRA-1 with feed arms at ±45° (left) and CIRA-2 with feed arms at ±30° (right).

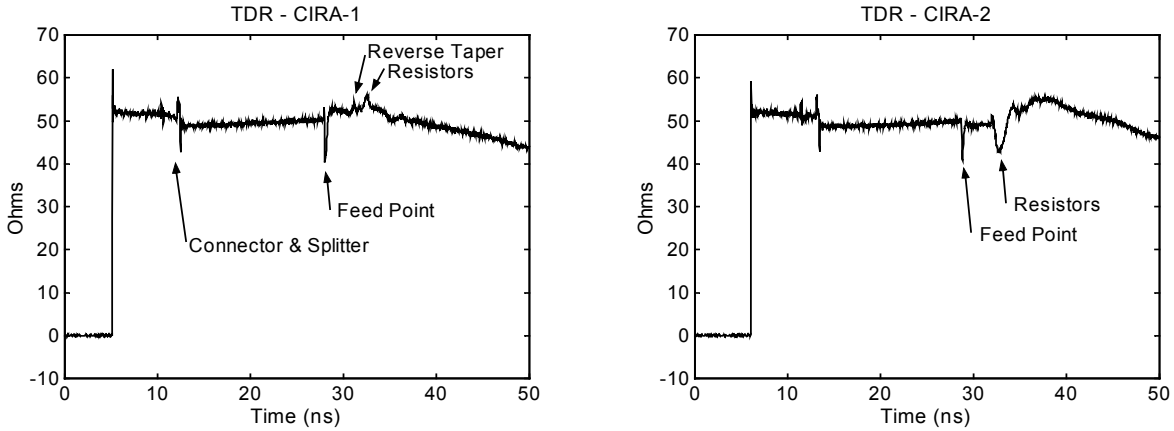

Figure 3.2. TDR of the CIRA-1 (left) and the CIRA-2 (right).

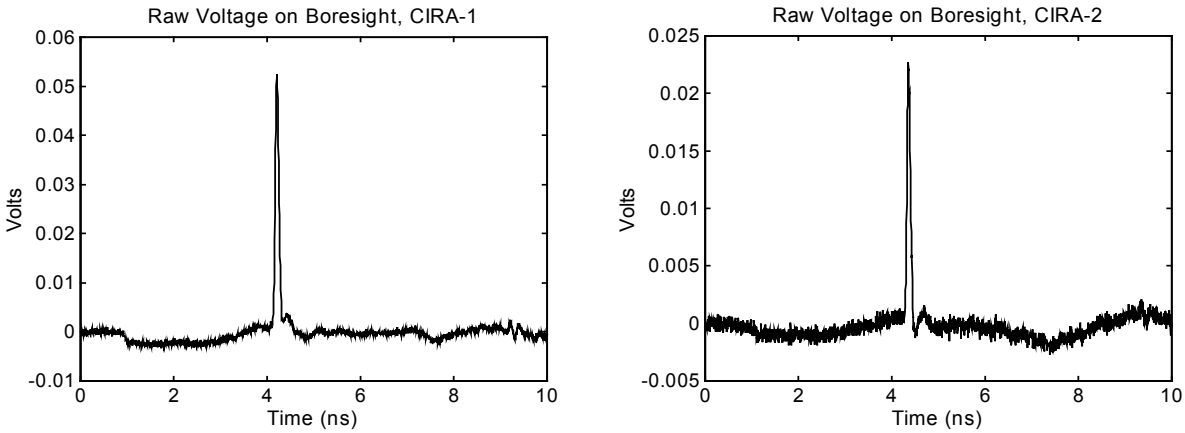

Figure 3.3. Raw Voltage, CIRA-1 with TEM-02-100, and CIRA-2 with TEM-01-50.

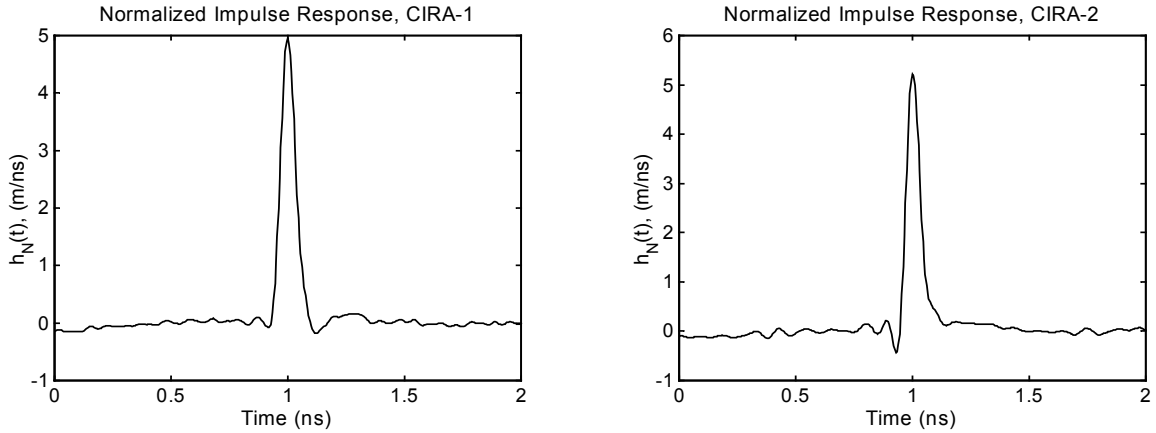

Figure 3.4. Normalized Impulse Response in the time domain.

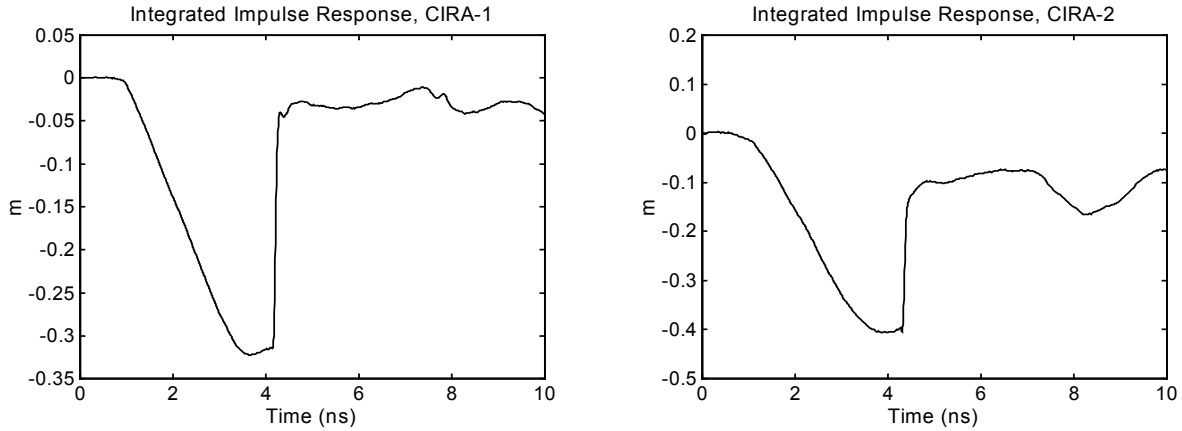

Figure 3.5. Integral of the Impulse Response (h_a).

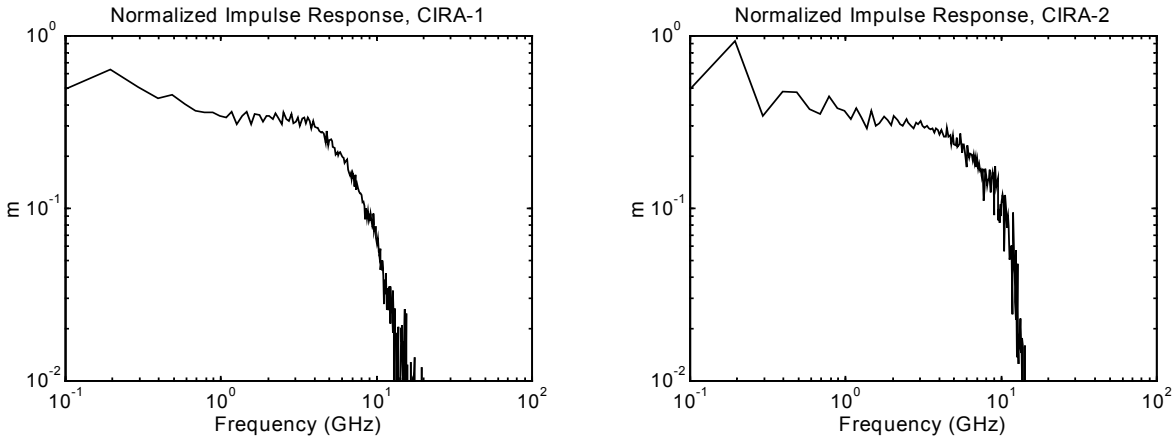

Figure 3.6. Normalized Impulse Response in the frequency domain.

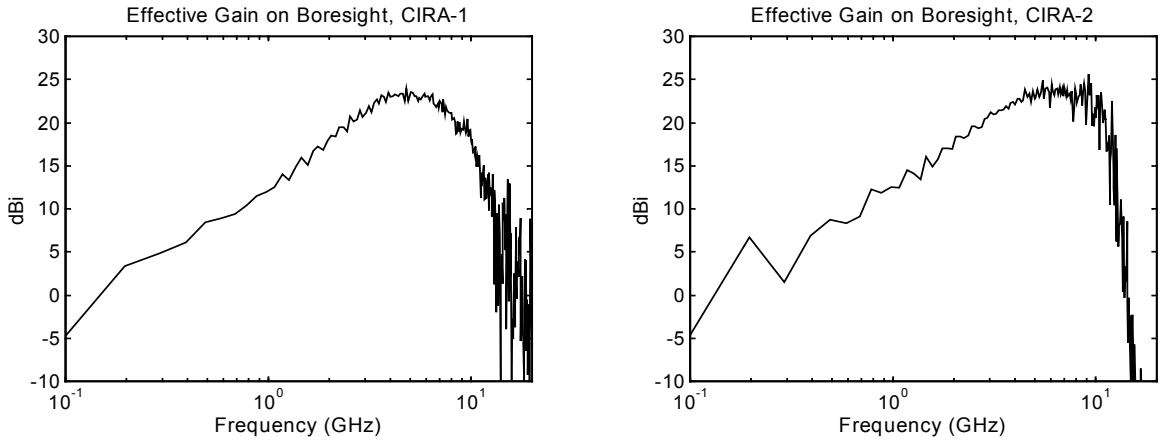

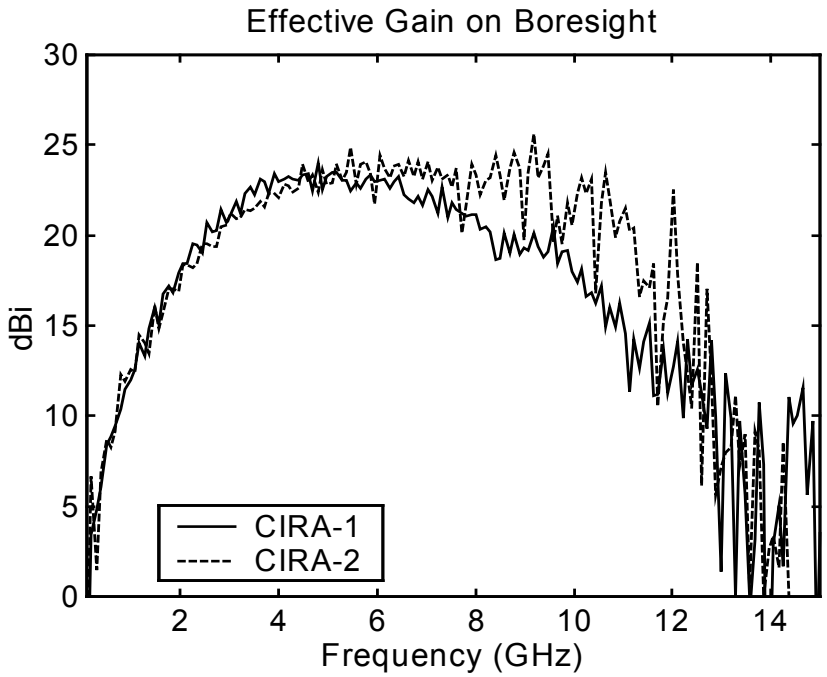

Figure 3.7. Effective gain on boresight.

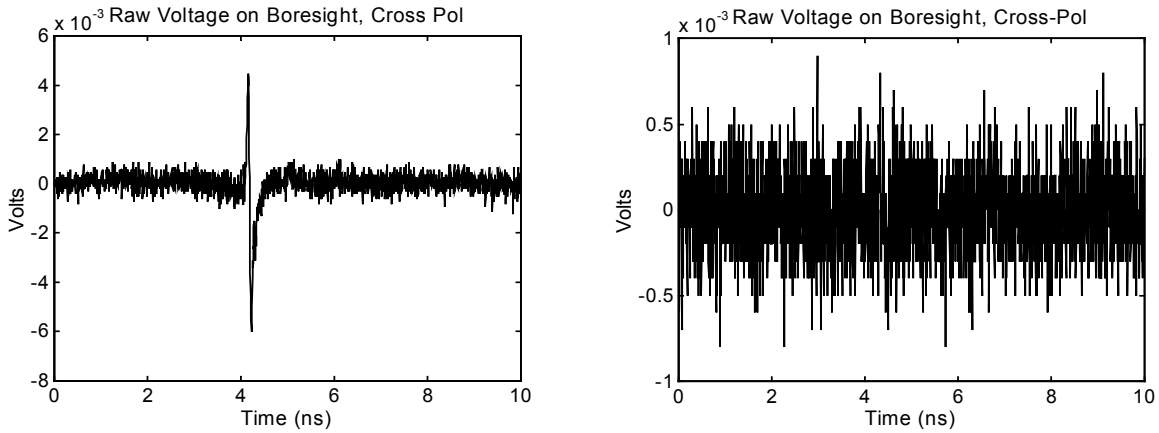

Figure 3.8. Crosspol response, CIRA-1 with TEM-02-100, and CIRA-2 with TEM-01-50.

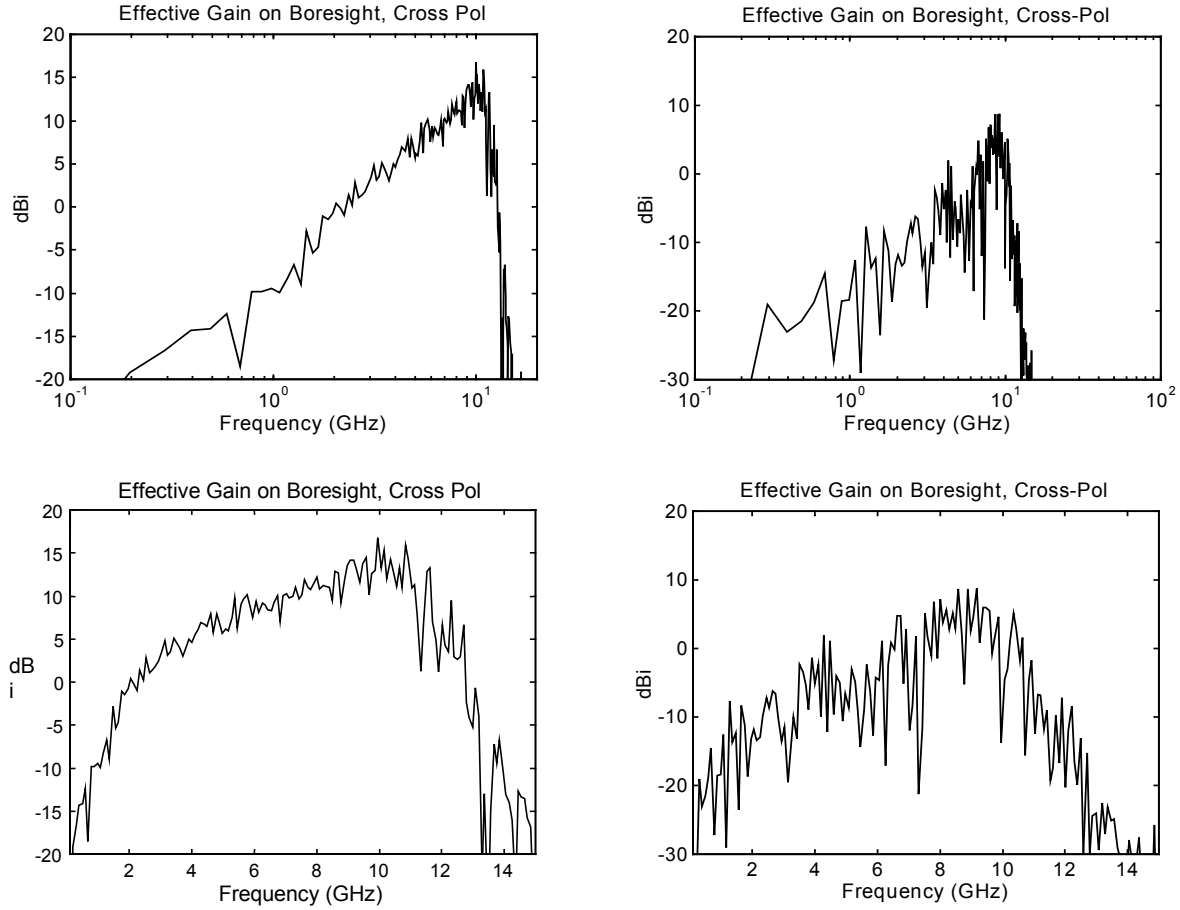

Figure 3.9. Cross polarization gain on boresight.

IV. Discussion

In two different antenna designs we have observed three effects from moving the feed arms to ±30° from the angle of dominant polarization. First, it increases the effective gain (standard antenna gain minus return loss). Second, it dramatically reduces the crosspolarized effective gain. Finally, it increases by a small amount the reflections seen on a TDR in the vicinity of the resistors.

So which antenna design is best? It may turn out that this will depend upon the intended application. In certain types of radar, a reflection from the antenna may be mistaken for actual signal from the target. In this case, the flatter TDR of the ±45° designs may be preferable. For most applications, however, increased effective gain and reduced crosspol gain will be the most important considerations. So for most applications, it appears that the ±30° designs will be preferred.

It is premature to render a final verdict, however. There are methods of reducing the TDR reflections of the ±30° designs by adjusting the resistors, and this will be described in a note to be published shortly. At this time, however, it appears to be unlikely that any ±30° design can ever be as flat as the CIRA-1 data shown in Figure 3.2.

In addition, there are methods of improving the crosspol rejection of the ±45° designs. It has been proposed by C. E. Baum [7] that the addition of either one or three dummy cables can improve the symmetry of an IRA, thereby reducing the crosspol. We will be trying this technique shortly, however, we note that both the ±30° designs and the ±45° designs may benefit from this technique.

In the final analysis, for most applications one will simply want to put the maximum field on target. In this case, the ±30° designs are preferred, as shown by the effective gain plots in Figures 2.7 and 3.7.

V. Conclusions.

The measurements presented in this report experimentally validate the optimization method developed by Tyo in [1]. The results of optimizing the 46 cm diameter IRA were outstanding. The increase in h_a from 0.120 to 0.143 is an improvement of 19%. The results for the CIRA were not as pronounced when h_a/a is considered, but the improvement in effective gain was still impressive.

The crosspol rejection for the IRA was increased by 11 dB and for the CIRA the increase was about 5 dB. Although crosspol rejection was not an optimization parameter, the reduction in the horizontal component of the feed arms was expected due to the reduced coupling of horizontal electric fields to the feed arms. Other factors such as symmetry are extremely important in reducing crosspol coupling to an IRA [7]. Although symmetry was not a major consideration in the redesign of the IRA, some changes such as the support at the feed point and the location of the feed coax did improve the symmetry of this antenna.

Patent Notice

A patent is pending on the Collapsible Impulse Radiating Antenna.

References

1. J. S. Tyo, Optimization of the Feed Impedance for an Arbitrary Crossed-Feed-Arm Impulse Radiating Antenna, Sensor and Simulation Note 438, November 1999.
2. C. E. Baum, Selection of Angles Between Planes of TEM Feed Arms of an IRA, Sensor and Simulation Note 425, August 1998.
3. E. G. Farr and C. E. Baum, Time Domain Characterization of Antennas with TEM Feeds, Sensor and Simulation Note 426, October 1998.
4. L. H. Bowen, E. G. Farr, and W. D. Prather, "A Collapsible Impulse Radiating Antenna," to appear in the proceedings of the 2000 Ultra-Wideband, Short-Pulse (EUROEM) Conference, held in Edinburgh, June 2000.
5. E. G. Farr, L. H. Bowen, G. R. Salo, J. S. Gwynne, C. E. Baum, W. D. Prather, and T. Tran, Studies of an Impulse Radiating Antenna and a Pulse Radiating Antenna Element for SAR and Target Identification Applications, Sensor and Simulation Note 442, March 2000.
6. L. H. Bowen, E. G. Farr, W. D. Prather, An Improved Collapsible Impulse Radiating Antenna, Sensor and Simulation Note 444, April 2000.
7. C. E. Baum, Symmetry in Single-Polarization Reflector Impulse Radiating Antennas, Sensor and Simulation Note 448, July 2000.
8. C. E. Baum, Some Topics Concerning Feed Arms of Reflector IRAs, Sensor and Simulation Note 414, October 1997.